

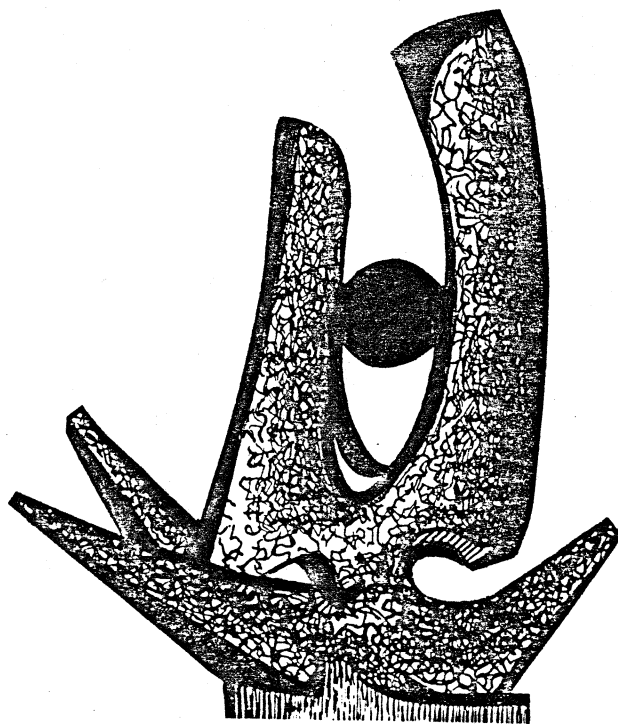
MICHIGAN STATE UNIVERSITY

CYCLOTRON LABORATORY

LIGHT PARTICLE CORRELATIONS IN INTERMEDIATE ENERGY  
HEAVY ION COLLISIONS

C.K. GELBKE

Invited talk given at the International Conference  
on Selected Aspects of Heavy Ion Reactions  
held at Saclay, May 3-7, 1982



APRIL 1982

LIGHT PARTICLE CORRELATIONS IN INTERMEDIATE ENERGY HEAVY ION COLLISIONS

C.K. Gelbke\*

Department of Physics  
 and  
 National Superconducting Cyclotron Laboratory  
 Michigan State University, East Lansing, MI 48824 USA

**Abstract:** Various light particle coincidence techniques will be reviewed that were employed to study the emission of energetic light particles in nucleus-nucleus collisions at energies above 10 MeV/nucleon. Several reaction mechanisms have been shown to contribute to the emission of energetic light particles, ranging from the sequential statistical decay of excited projectile residues, direct breakup and knock-out reactions, to multistep emission processes that can be rather well described in terms of the concept of local thermal equilibrium.

1. Introduction

Nucleus-nucleus collisions at energies significantly above the Coulomb barrier are generally accompanied with the dissipation of large amounts of the incident kinetic energy into more complex degrees of freedom. As a consequence, the emerging nuclei are highly excited and decay by the emission of light particles and  $\gamma$ -rays or by fission. At low energies, the emission of light particles occurs predominantly after full statistical equilibrium of the intrinsic degrees of freedom has been attained by the primary reaction products. With increasing energy, particle emission prior to the attainment of full statistical equilibrium is expected to become important.

Some of the characteristics of light particle energy spectra observed at beam energies above 10 MeV per nucleon are illustrated in Fig. 1. Part a of the figure

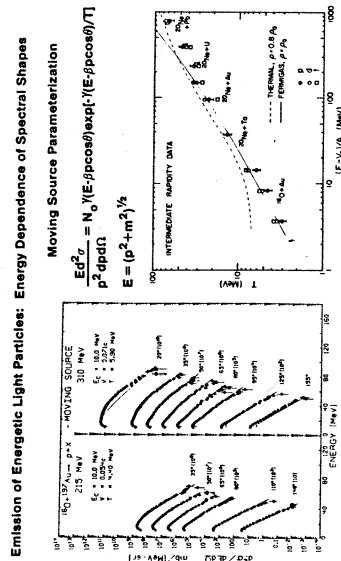


FIG. 1. a) Proton cross sections measured<sup>1)</sup> for the reaction  $^{197}\text{Au}(^{16}\text{O}, p)$  at 215 and 310 MeV. The solid lines correspond to thermal emission from a moving source. b) Energy dependence of moving source temperatures<sup>2)</sup> extracted from single-particle inclusive cross sections.

shows the cross sections measured<sup>1)</sup> for the reaction  $^{197}\text{Au}(^{16}\text{O}, p)$  at  $E/A = 13.4$  and 19.4 MeV. The energy spectra are smooth, structureless distributions which, at forward angles, extend to about four times the incident energy per nucleon. With increasing detection angle, the cross sections decrease and the slopes of the energy spectra become steeper. The cross sections can be rather well described in terms of a Maxwellian distribution observed in a rest frame that moves with a velocity intermediate between target and projectile, as is shown by the solid lines. Part b of the figure shows the dependence<sup>2)</sup> of the moving source temperatures on the kinetic energy per nucleon above the Coulomb barrier. The temperatures exhibit a rather smooth energy dependence which is in good agreement with the expectations from a thermal model if one assumes that thermal equilibrium is not established over the entire projectile-target composite but rather in a localized region that is of the order of magnitude of the "participant" zone corresponding to the region of geometrical overlap of the colliding nuclei.

A variety of reaction mechanisms have been suggested to lead to the emission of energetic light particles, ranging from direct knock-out and breakup reactions to multistep intranuclear cascade processes leading to the attainment of local thermal equilibrium. It should be clear that single particle inclusive measurements are, very often, not restrictive enough to discriminate between different models. The main reason for this lack of discrimination is the dominance of kinematic and phase space effects on the single particle inclusive observables. Coincidence experiments of various kinds are more restrictive and allow the examination of certain regions of phase space in significant detail. In the following, several light particle coincidence experiments will be reviewed with an emphasis on investigations of reactions that involve the emission of energetic light particles which do not result from compound nucleus decay.

2. Sequential Decay

Strongly damped nucleus-nucleus collisions at incident energies of only a few MeV per nucleon above the Coulomb barrier are essentially binary reactions with two highly excited primary reaction products in the exit channel. These primary reaction products decay in flight on a time scale that is large as compared to the nuclear collision time. Such sequential decays can be described within the framework of the statistical theory of compound nucleus decay. Measurements of energy and angular correlations of the decay products can then give valuable information about the excitation energies and angular momenta of the primary reaction products. Two examples of such measurements shall suffice for illustration.

Hilscher et al.<sup>3)</sup> have measured neutrons in coincidence with projectile residues for  $^{56}\text{Fe}$  induced reactions on  $^{157}\text{Ho}$  at  $E_{\text{lab}} = 476$  MeV. By observing that neutron evaporation from projectile and target residues is focussed into different directions (see Fig. 2a) they were able to extract the average temperatures of projectile and target residues (see Fig. 2b). Within the experimental uncertainties, the temperatures of the two primary reaction products were found to be identical, indicating that thermal equilibrium is reached during the collision stage of the interaction. No evidence for preequilibrium emission of neutrons was found in this experiment.

Information about the spin distributions of the primary reaction products can be obtained by measuring the angular correlations of the decay products. As an example, Fig. 3a shows the measured<sup>4)</sup> out-of-plane correlation of alpha particles emitted from target residues in  $^{40}\text{Ar}$  induced reactions on  $^{93}\text{Nb}$  at 400 MeV. The results are consistent with angular momentum transfers that correspond to rigid rotation of the dinuclear complex during the collision (sticking limit, see Fig. 3b).

### 3. Light-Particle Projectile-Residue Coincidences

Early searches for nonequilibrium light particle emission in nucleus-nucleus collisions employed coincidence measurements between projectile residues and energetic alpha particles. In the absence of orbiting, Fermi jets should lead to the preferential emission of projectile residues and light particles on opposite sides of the beam axis, whereas emission on the same side should occur for breakup or sequential decay reactions. If negative deflection angles occur, these correlations should be reversed for Fermi-jets or fast breakup reactions but not for sequential decay processes, see Fig. 4 for illustration. Characteristic shadowing effects<sup>6)</sup> due to the reabsorption of light particles by the surrounding cold nuclear matter have been predicted for the emission from "hot spots".

Up to the present, none of the correlations that were predicted for Fermi-jets or hot spots could be positively identified. Instead, the observed angular correlations were consistent with the simpler processes of projectile breakup or sequential decay. Angular correlations observed<sup>7)</sup> for the quasi-elastic reactions  $^{19}\text{Au}(^{16}\text{O},^{12}\text{C})$  and  $^{208}\text{Pb}(^{16}\text{O},^{12}\text{C})$  at  $E/A = 19.4$  MeV are shown in Fig. 4. These correlations are strongly peaked but not symmetric about the direction of the detected heavy ion. They are, however, not inconsistent with the rather trivial process of sequential decay, for which large asymmetries about the direction of the heavy ion can result from the recoil imparted on the heavy ion by the decay of the parent nucleus. The detailed shapes of angular correlations from sequential decay of projectile residues have been shown<sup>7)</sup> to depend strongly on the angular and excitation energy distributions of the primary fragments. This fact makes the distinction between fast breakup processes and slow sequential decay processes via angular correlation measurements extremely cumbersome, because these two reaction mechanisms correspond to rather similar kinematic situations. Sequential decay processes can only be ruled out in a convincing manner if the resulting angular correlations can be demonstrated to exhibit sizeable left-right or forward-backward asymmetries in the rest-frame of the primary fragments. Care has to be taken that the comparisons are made for a fixed scattering angle of the primary fragments<sup>7)</sup> which generally have rapidly varying angular distributions.

MSUK-82-100

### Neutron Emission in Strongly Damped Collisions

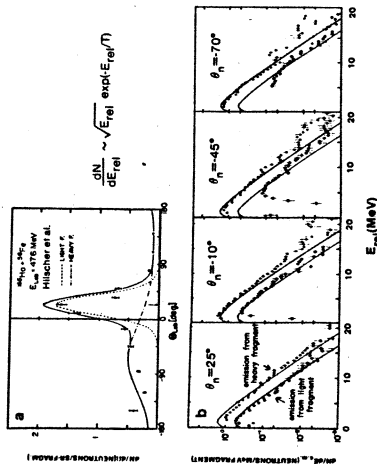


FIG. 2. Neutron cross sections measured<sup>8)</sup> in coincidence with projectile residues in strongly damped collisions of  $^{56}\text{Fe}$  and  $^{16}\text{O}$  at 476 MeV. a) Angular correlation; the detection angle of the projectile residue is marked by an arrow. b) Energy spectra in restframes of projectile and target residues.

Fragment Spin Distributions from Sequential Decay:

$$P(J) \sim \exp\left[-\frac{J(J+1)}{2\sigma^2}\right]$$

Out-of-Plane Correlation

$$W(\theta) \sim \exp\left[-\frac{C}{2\sigma^2} \cos^2\theta\right]$$

$$C = \frac{h^2}{2I} \frac{\mu^2}{\mu^2 + \mu_R^2}$$

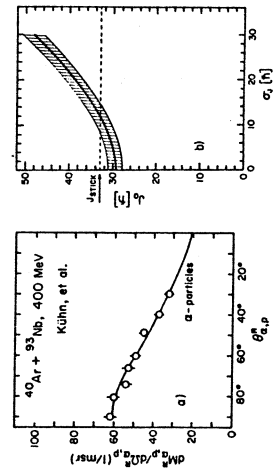


FIG. 3. a) Out-of-plane angular correlations<sup>9)</sup> of sequentially emitted alpha particles for  $^{40}\text{Ar}$  induced reactions on  $^{93}\text{Nb}$  at 400 MeV. b) Mean values and variances of angular momentum transfer consistent<sup>9)</sup> with the angular correlations shown in part a.

MSUK-82-109

### Heavy-Ion Alpha-Particle Angular Correlations

Fermi-Jets Fast Breakup Sequential Decay

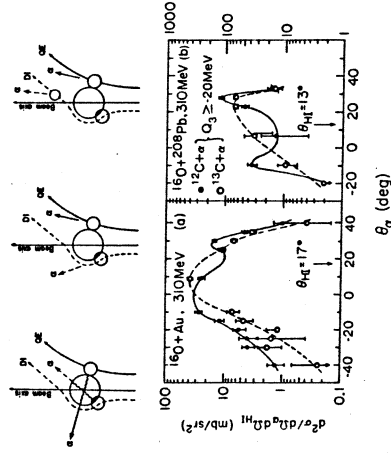


FIG. 4. Schematic illustration of light-particle projectile-residue angular correlations expected for different reaction mechanisms. Angular correlations measured<sup>7)</sup> for quasi-elastic  $^{16}\text{O},^{12}\text{C}$  reactions on  $^{197}\text{Au}$  and  $^{208}\text{Pb}$  at 310 MeV.

Most heavy-ion light-particle coincidence measurements reported up to now were only performed for a limited set of heavy ion detection angles with no attempt to obtain a set of measurements corresponding to a fixed scattering angle of the primary fragments. With these limitations, most of the experiments found no contradiction to the assumption of sequential decay processes.

Sequential decay processes involve, by definition, the excitation and decay of individual states of the parent nucleus which can be identified in the spectrum of relative kinetic energy,  $E_{rel}$ , of the decay products. The observation of sharp states in the spectrum of relative kinetic energy is, therefore, an indication for a sequential decay process. The occurrence of relative kinetic energies, on the other hand, that cannot be associated with a state of the parent nucleus can then be taken as evidence for a fast breakup process. The method can, however, yield no definitive conclusions if the measured relative kinetic energies correspond to the continuum region of the spectrum where individual states can no longer be resolved.

Several experiments have been performed with sufficient energy and angular resolution to clearly establish the importance of sequential decay processes for the production of energetic alpha particles at forward angles<sup>11)</sup>. All of these investigations have, however, also presented evidence for fast non-sequential light-particle emission processes. Unambiguous proof for such processes has been obtained from Li induced reactions<sup>8, 11)</sup> where relative kinetic energies of the two coincident particles have been measured that could not result from the quasi-free decay of the corresponding parent nucleus. For the ( $^7\text{Li}, t$ )  $\alpha$  reaction, the threshold lies at 2.5 MeV with the first excited state above threshold lying at 4.6 MeV, see Fig. 5. Sequential decay processes cannot produce relative kinetic energies below 2.1 MeV. These decay energies have, however, been identified experimentally<sup>11)</sup> as is shown in Fig. 5.

A recent high resolution study of the ( $^{16}\text{O}, ^{12}\text{C}$ ) reaction at  $E/A = 8.8$  MeV has revealed<sup>10)</sup> at least two reaction mechanisms contributing to the breakup of the projectile: (i) a "coherent" process which excites the projectile to states whose structure is related to the ground state via a multipole operator and (ii) "incoherent" processes that contain resonant contributions corresponding to specific excited states in the projectile and also nonresonant contributions to the continuum. It was suggested that the dominant incoherent process corresponds to the quasi-free scattering of the  $\alpha$  or  $^{12}\text{C}$  constituents by the target, i.e. the direct breakup of the projectile.

Sequential and Non-Sequential Breakup (Shottor et al.)

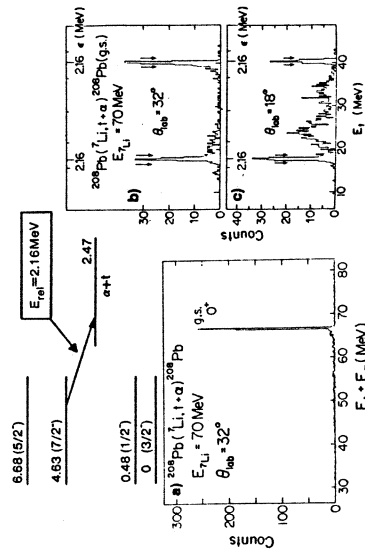


FIG. 5. Experimental proof<sup>11)</sup> for the occurrence of sequential and non-sequential breakup for quasi-elastic  $^{208}\text{Pb}(^7\text{Li}, t)$  reactions at 70 MeV.

Heavy-ion alpha-particle coincidence measurements for processes involving large negative values of the three-body reaction Q-value revealed a remarkable lack of correlation between the outgoing particles.<sup>9, 12, 13)</sup> The coincidence cross sections were shown to be proportional to the singles cross sections,  $\sigma_{12}^{-1}\sigma_{102}$ . This observation was taken as evidence that a major part of the energetic light particles is produced at an early stage of the reaction - a conclusion that was also arrived at from fission coincidence studies,<sup>14, 15)</sup> see section 5.

#### 4. Light-Particle Gamma-Ray Coincidences

Clear proof for the overall importance of fast, non-sequential light particle emission processes has been obtained from the detection of energetic light particles in fusion-like reactions for which no projectile residues emerge in the exit channel. These reactions have been investigated primarily with  $\gamma$ -ray or fission coincidence techniques.

By detecting discrete  $\gamma$ -rays in coincidence with energetic light particles it is possible to determine the amount of charge that is absorbed by the target during the reaction and, therefore, exclude the emission of projectile residues in the exit channel. The results of Yamada et al.<sup>16)</sup>, obtained for  $^{14}\text{N}$  induced reactions on  $^{132}\text{Sm}$  at 135 MeV, are shown in Fig. 6. Part a of the figure shows the light particle spectra observed in coincidence with any  $\gamma$ -ray. Part b of the figure shows the proton spectra measured for the p6n and p7n exit channels, which clearly exhibit high energy components that cannot be explained in terms of the statistical decay of the compound nucleus. The detailed shapes of the energy spectra depend on the exit channel, indicating a rather high degree of phase space selectivity of this coincidence technique.

The connection to single particle inclusive spectra may be established by summing over many exit channels. Figure 7 shows the summed neutron spectra observed<sup>17)</sup> for the xn and  $\alpha$ xn exit channels of the  $^{16}\text{O} + ^{154}\text{Sm}$  reaction at  $E_{lab} = 152$  MeV. Two components are apparent in these spectra. The low energy component is due to neutron evaporation from the compound nucleus as shown by the dashed curves. The high energy component is associated with precompound emission. It can be rather well described in terms of thermal emission from a moving source as is shown by the dot-dashed curves in part a of the figure (see also Fig. 1). The PPP model of ref. 18, on the other hand, fails to reproduce the high energy tails of the energy spectra, especially at larger angles, as is shown by the dot-dashed curves in part b of the figure.

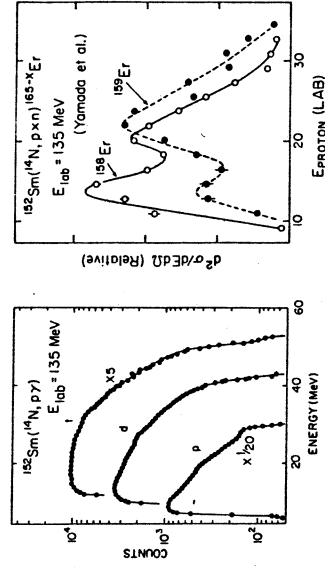


FIG. 6 Light particle spectra measured<sup>16)</sup> for  $^{152}\text{Sm}(^{14}\text{N}, p\gamma)$  reactions at 135 MeV. a) Spectra observed in coincidence with any  $\gamma$ -ray. b) Spectra observed in coincidence with known transitions in  $^{159}\text{Er}$  and  $^{165}\text{Er}$ .

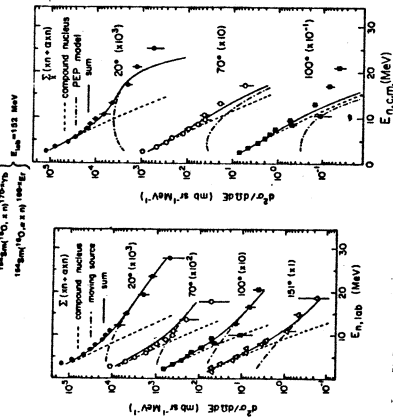


FIG. 7. Summed neutron yields observed<sup>17)</sup> in coincidence with  $\gamma$ -rays identifying xn and  $\alpha$ xn exit channels for  $^{16}\text{O}$  induced reactions on  $^{152}\text{Sm}$  at 152 MeV. a) Comparison with moving source fits. b) Comparison with PEP model<sup>18)</sup>.

According to the classical model of ref. 19, the emission of energetic light particles should occur for a rather narrow range of entrance channel partial waves  $l_{\text{fus}} < l < l_{\text{crit}}$  that lead to "incomplete fusion" reactions. (Here,  $l_{\text{fus}}$  denotes the maximum angular momentum for complete fusion and  $l_{\text{crit}}$  is the maximum angular momentum for which the two nuclei can still reach the "critical distance" corresponding to the sum of their half-density radii.) These expectations have been confirmed<sup>20)</sup> for the emission of energetic alpha particles in  $^{16}\text{O}$  ( $^{16}\text{O}, \alpha$ ) and  $^{16}\text{O}$  ( $^{16}\text{O}, \alpha n$ ) reactions at 142 MeV. Rather low sidefeeding into the rotational bands of  $^{151,152}\text{Dy}$  was observed in coincidence with energetic alpha particles, corresponding to a narrow window at high angular momentum for the occurrence of incomplete fusion, see Fig. 8.

$^{146}\text{Nd} (^{16}\text{O}, \alpha x n) ^{158-2}\text{Dy}$ ,  $E_{\text{lab}} = 142 \text{ MeV}$

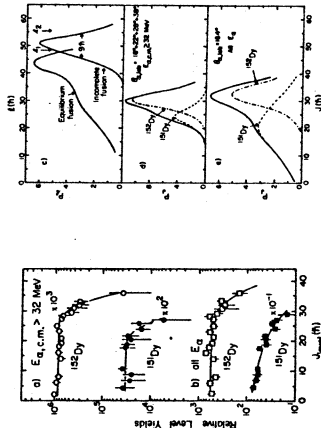


FIG. 8. Evidence<sup>20)</sup> for a narrow window at high angular momentum for the incomplete fusion reaction  $^{16}\text{O} (^{16}\text{O}, \alpha n)$  at 142 MeV. a) Relative level yields observed in coincidence with energetic alpha particles. b) Relative level yields observed in coincidence with any alpha particle. c-e) Deduced angular momentum distributions.

5. Linear Momentum Transfer from Correlated Fission Fragments

For fissionable target nuclei, information about the linear momentum transfer to the target residue may be obtained by measuring the folding angle  $\theta$  between the two fission fragments resulting from the decay of the target residue.  $^{137}\text{Ba} (5.21) \text{ As}$  is illustrated in Fig. 9, increasing momentum transfer to the target residue corresponds to smaller folding angles.

This technique has been used  $^{14,15,21)}$  to study the emission of energetic light particles in  $^{16}\text{O}$  induced reactions on  $^{238}\text{U}$  at  $E/A = 19.4 \text{ MeV}$ . The inclusive folding angle distribution shown in Fig. 9 clearly exhibits two components. The high momentum transfer component, centered around  $\theta_{\text{AB}} \approx 148^\circ$ , corresponds to fusion-like or "central" collisions and the low momentum transfer component, centered around  $\theta_{\text{AB}} \approx 173^\circ$ , corresponds to "peripheral" collisions, such as inelastic scattering, breakup or transfer reactions, for which a projectile residue emerges in the exit channel (compare the folding angle distribution measured in coincidence with projectile residues, Li, Be, ..., O, close to the grazing angle).

By measuring light particles in coincidence with two fission fragments it is possible to compare the characteristics of light particle emission in transfer-like and fusion-like reactions. The main results of such an investigation  $^{17,18,21)}$  are summarized in Fig. 10. At forward angles, energetic light particles are emitted both in fusion-like ( $\theta_{\text{AB}} < 160^\circ$ ) transfer-like ( $\theta_{\text{AB}} > 160^\circ$ ) collisions. A relatively larger fraction of alpha particles is emitted in peripheral collisions at forward angles as compared to the smaller contribution of peripheral reactions to the emission of energetic hydrogen isotopes. Rather similar energy spectra are observed for the two processes, suggesting that energetic light particles are emitted at an early stage of the reaction. At larger angles, energetic light particles are predominantly emitted in fusion-like reactions (for which the sequential decay of projectile residues is excluded, since nearly the entire projectile momentum is absorbed by the target residue).

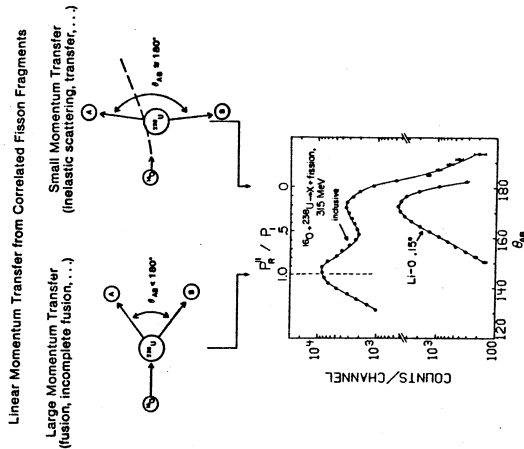


FIG. 9. Folding angle distributions observed  $^{14,15,21)}$  for  $^{16}\text{O}$  induced reactions on  $^{238}\text{U}$  at 310 MeV.

Energetic Light Particles Emitted in Low and High Momentum Transfer Collisions

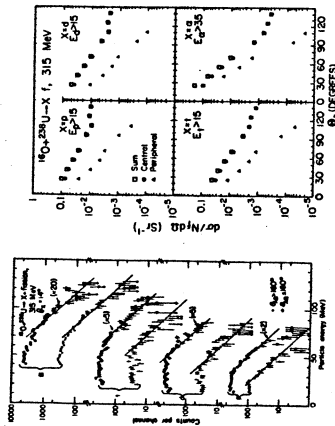


FIG. 10. Energy spectra<sup>14,21</sup>, part a, and angular distributions<sup>15</sup>, part b, of light particles observed in fusion-like ("central",  $\theta_{AB} < 160^\circ$ ) and transfer-like ("peripheral",  $\theta_{AB} > 160^\circ$ ) reactions of  $^{16}\text{O} + ^{16}\text{O}$  at 310 MeV.

Finally it should be pointed out that the fission correlation technique is expected to impose only minor phase space constraints on the reaction. As a consequence, the coincident light particle spectra exhibit the main characteristics of the single particle inclusive cross sections, i.e. they can be fit with the moving source parameterization and the spectra of composite light particles are connected to the proton spectra via a coalescence relation<sup>15</sup>.

### 6. Light Particle Correlations

Light particle inclusive cross sections at sufficiently large transverse momenta can be rather well described by the concept of local statistical equilibrium, compare Fig. 1. According to this hypothesis, no dynamical correlations should exist between two coincident light particles; the only remaining correlations should result from the phase space constraints imposed by the conservation laws (finite particle number effect) or from final state interactions as the particles leave the statistical ensemble.

Up to the present, light particle correlation studies were stimulated by two motivations: (i) test the statistical assumption and search for possible dynamical correlations that could provide clues about the reaction mechanism; (ii) take advantage of final state interactions and try to obtain information about the space-time extent of the emitting ensemble.

In-plane light particle correlations have been investigated<sup>22</sup> for  $^{16}\text{O}$  induced reactions on  $^{27}\text{Al}$  and  $^{197}\text{Au}$  at  $E/A = 19.4$  MeV. Rather similar energy spectra were observed in the single-particle and two-particle inclusive measurements indicating that the assumption of statistical emission is not strongly violated, see Fig. 11. A more sensitive test for two-particle correlations may be obtained from the correlation function  $g_{12}/g_1^2$  defined by the ratio of coincidence and single yields. For the  $^{16}\text{O} + ^{27}\text{Al}$  reaction<sup>22</sup>, the measured correlation exhibits

Comparison of Single-particle and Two-particle Inclusive Spectra:

- single-particle inclusive
- two-particle inclusive,  $\theta_2 = -30^\circ$
- - - two-particle inclusive,  $\theta_2 = +30^\circ$

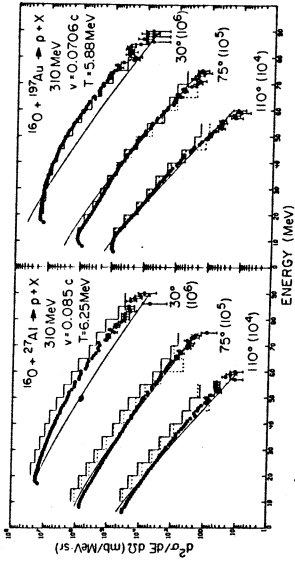


FIG. 11. Comparison of single-particle and two-particle inclusive energy spectra observed<sup>22</sup>) for  $^{16}\text{O}$  induced reaction on  $^{27}\text{Al}$  and  $^{197}\text{Au}$  at 310 MeV.

Phase Space Constraints from Conservation Laws (Finite Particle Number Effects)

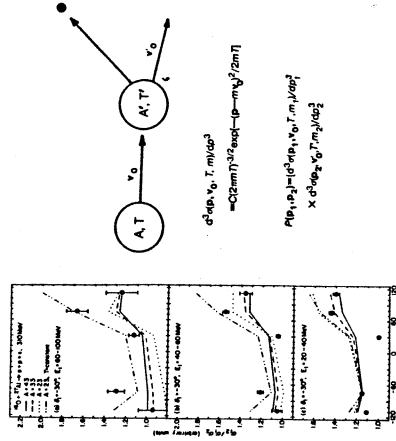


FIG. 12. Ratio of coincidence and singles yields,  $g_{12}/g_1^2$ , measured<sup>22</sup>) for the reaction  $^{16}\text{O} + ^{27}\text{Al}$  at 310 MeV. The curves demonstrate the constraints imposed by energy and momentum conservation if the emission occurred from a moving source consisting of A nucleons.

$$\frac{\sigma(\theta_1, \theta_2)}{\sigma(\theta_1) \sigma(\theta_2)} = \frac{1}{4} (1 + \rho_{\theta_1, \theta_2}^2) \quad \rho_{\theta_1, \theta_2} = 0 \text{ for } \theta_1 \neq \theta_2$$

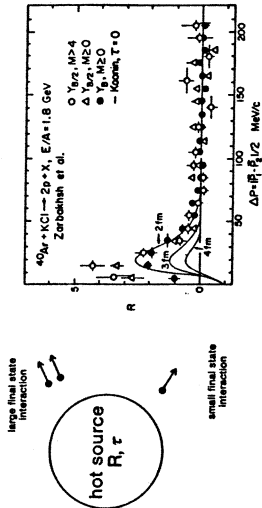


FIG. 14. Proton-proton correlations at small relative momenta measured<sup>(28)</sup> for <sup>40</sup>Ar induced reactions on KCl at E/A = 1.8 GeV. The curves were calculated with the model of ref. 27, with the values of the mean square radii  $r_0$  given in the figure. The equivalent sharp sphere radii are given by  $R_0 = 1.58 r_0$ .

The random emission of light particles from a finite size source will, in general, still exhibit measurable correlations due to final state interactions or quantum statistical symmetries that affect the wavefunctions of particles that are emitted within small space-time intervals. These correlations can provide useful information about the space-time extent of the emitting sources.<sup>(27)</sup> At present, the final state interactions between two coincident light particles have been taken into account quantitatively for the case of proton-proton correlations<sup>(27)</sup>; however, little is known about the effects of the long range Coulomb interaction between the target residue and the emitted light particles.

In Fig. 14, two-proton correlations measured<sup>(28)</sup> for the reaction <sup>40</sup>Ar + KCl at E/A = 1.8 GeV are compared to the model calculations of ref. 27. The small size of the sharp sphere radius,  $R_0 = 2.4$  fm, which was extracted for nucleon emission at intermediate rapidities using a high multiplicity trigger ( $\frac{1}{2} Y_B, M > 4$  in the figure) is even smaller than expected from simple geometrical models; this striking result is not understood, at present.

### 7. Summary and Conclusion

Light particle coincidence experiments performed during the last few years have provided valuable insights into the reaction mechanisms that contribute to the emission of energetic light particles in nucleus-nucleus collisions. Experiments have been performed in the energy ranges below E/A ≈ 20 MeV and above E/A ≈ 400 MeV, leaving the entire range from a few ten to a few hundred MeV per nucleon for future research.

At low energies, light-particle projectile-residue coincidence experiments have identified the processes of sequential decay and, in some instances, of fast breakup. The clear distinction between these two reaction mechanisms is, in general, rather cumbersome, if not impossible, when the relative kinetic energies between the coincident particles correspond to the continuum region of the energy

variations of up to 50%, see Fig. 12. These variations are comparable in magnitude to the ones that are imposed by energy and momentum conservation on a finite ensemble, as is shown by the schematic moving source calculations in Fig. 12. The detailed shapes of the experimental correlations are not reproduced by these schematic calculations. This is not surprising, since the calculations ignore the effects of impact parameter averaging and possible contributions from sequential decay and knockout reactions.

If quasi-free knockout reactions are important in nucleus-nucleus collisions, an enhancement of the coincident proton-proton cross section will occur at the location corresponding to the free nucleon-nucleon kinematics. This enhancement will be broadened by the nucleon Fermi velocity distribution and there will be a damping due to a combinatorial background resulting from uncorrelated nucleon-nucleon scatterings. Such processes have been identified for proton-nucleus collisions<sup>(3)</sup> at 800 MeV and for collisions between lighter nuclei<sup>(24)</sup> at E/A = 400 and 800 MeV, as is shown in Fig. 13. Part a of the figure<sup>(23)</sup> gives a comparison of single-particle inclusive and two-particle inclusive proton spectra measured for in- and out-of-plane geometries at  $\theta_{lab} = 40^\circ$  for the reaction p + C at 800 MeV. The quasi-free scattering component is clearly identified in the coincidence spectrum measured in coplanar geometry. Part b of the figure gives the ratio of in- and out-of-plane coincidence yields for the C + C reaction<sup>(24)</sup> at E/A = 800 MeV, showing an enhancement of the inplane cross sections which is partly due to the knockout component but is likely to contain contributions from multiple scattering components.<sup>(24)</sup> Also included in the figure are the calculations from a geometrical phase space model<sup>(25, 26)</sup> which reproduce the observed correlations rather well.

### Knock-Out Contributions

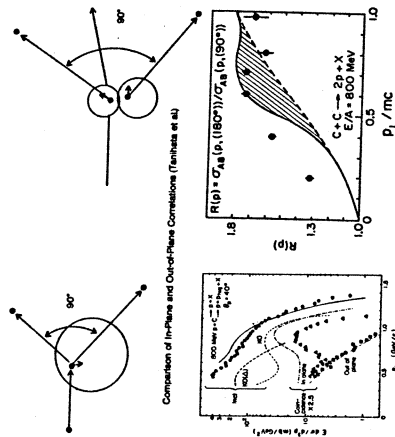


FIG. 13. Evidence for knock-out processes.<sup>(25)</sup> a) Single-particle and two-particle inclusive spectra measured<sup>(1)</sup> for proton induced reactions on C at 800 MeV. b) Ratio of in- and out-of-plane coincidence yields<sup>(24)</sup> for the reaction C + C + 2p + X at E/A = 800 MeV. The calculations correspond to the geometric phase space model of ref. 26. The shaded area in part b corresponds to the calculated knockout contribution.

spectrum of the parent nucleus. More exotic processes like Fermi Jets or emission from hot spots have not been identified in such experiments - perhaps because of the rather gentle nature of grazing collisions which might make sequential decay processes and breakup reactions the dominant aspects of these reactions.

Clear evidence for precompound emission processes in nucleus-nucleus collisions at energies between  $E/A \approx 10$ -20 MeV was obtained from the measurement of energetic light particles in coincidence with discrete  $\gamma$ -rays or correlated fission fragments. The energy spectra of precompound light particles measured in these experiments could be rather well described in terms of a thermal spectrum in a moving rest frame, suggesting that local thermal equilibrium may be attained in these reactions.

Rather similar energy spectra were measured in single- and two-proton inclusive experiments at  $E/A = 19.4$  MeV indicating that the assumption of local thermal equilibrium is not strongly violated. The observed variations of the proton-proton correlation function were comparable in magnitude to the ones that may be imposed by energy and momentum conservation for a finite ensemble. Proton-proton correlations measured for C + C and Ne + NaF collisions at  $E/A$  400 MeV have, on the other hand, provided clear evidence for non-thermal knockout contributions to the light particle production cross sections.

By measuring light particle correlations at small relative momenta it has been possible to obtain first information about the space-time extent of the emitting source. Although, at present, there are still some open theoretical problems concerning the interpretation of these data this technique offers a unique probe to investigate the extent of localized thermal sources formed in nucleus-nucleus collisions.

Finally, I want to conclude by noting that particle correlation experiments in nucleus-nucleus collisions are still in their infancy stage of development. They have already provided valuable insights into the reaction mechanisms that contribute to non-compound light particle emission. As the theoretical model predictions become more specific these investigations will provide more stringent constraints to our interpretation of nucleus-nucleus reactions than single-particle inclusive measurements. At the same time a better understanding of the "background" due to pure phase space will be imperative, especially, when we move on from the investigation of two-particle correlations to multiparticle correlation studies.

This material is based upon work supported by the National Science Foundation under Grant No. Phy 80-17605.

#### References

- \* Alfred P. Sloan Fellow
1. T.C. Aves, G. Poggi, S. Saini, C.K. Gelbke, R. Legrain, and G.D. Westfall, Phys. Lett. 103B (1981) 417.
2. G.D. Westfall, B.V. Jacak, N. Anantaraman, M.V. Curtin, G.M. Crawley, C.K. Gelbke, B. Hasselquist, W.G. Lynch, D.K. Scott, M.B. Tsang, M.J. Murphy, T.J.M. Symons, R. Legrain, and T.J. Majors, Michigan State University preprint, 1982.
3. D. Hilscher, J.R. Birkelund, A.D. Hoover, W.U. Schröder, W.W. Wilcke, J.R. Huizenga, A.C. Mignerey, K.L. Wolf, H.F. Breuer, and V.E. Viola, Jr., Phys. Rev. C20 (1979) 576.
4. W. Kühn, R. Albrecht, H. Damjantschitsch, H. Ho, R.M. Rönning, J. Slemmer, J.P. Wurm, I. Rode, and P. Scheibling, Z. Phys. A298 (1980) 95.
5. D.H.E. Gross and J. Wilczynski, Phys. Lett. 67B (1977) 1.
6. P.A. Gottschalk and M. Westrom, Phys. Rev. Lett. 39 (1977) 1250, Nucl. Phys. A314 (1979) 232.
7. M. Bini, C.K. Gelbke, D.K. Scott, T.J.M. Symons, P. Doll, D.L. Hendrie, J.L. Laville, J. Mahoney, M.C. Mermaz, C. Olmer, K. van Bibber, and H.H. Wieman, Phys. Rev. C22 (1980) 1945.
8. H. Gemmeke, B. Deluigi, D. Scholz, and D. Lassen, Phys. Lett. 96B (1980) 47.
9. J. van Driel, S. Gonggrijp, R.V.F. Janssens, R.H. Siemssen, K. Siwek-Wilczynska, and J. Wilczynski, Phys. Lett. 98B (1981) 351.

10. W.D. Rae, A.J. Cole, A. Dacal, R. Legrain, B.G. Harvey, J. Mahoney, M.J. Murphy, R.G. Stokstad, and I. Tserruys, Phys. Lett. 105B (1981) 417.
11. A.C. Shotter, A.N. Bice, J.M. Wouters, W.D. Rae, and J. Cerny, Phys. Rev. Lett. 46 (1981) 12.
12. R.K. Bhowmik, E.C. Pollacco, N.E. Sanderson, J.B.A. England, and G.C. Morrison, Phys. Rev. Lett. 43 (1979) 619.
13. R.K. Bhowmik, E.C. Pollacco, J.B. England, G.C. Morrison, and N.E. Sanderson, Nucl. Phys. A363 (1981) 516.
14. T.C. Aves, C.K. Gelbke, B.B. Back, A.C. Mignerey, K.L. Wolf, P. Dyer, H. Breuer, and V.E. Viola, Jr., Phys. Lett. 87B (1979) 43.
15. T.C. Aves, G. Poggi, C.K. Gelbke, B.B. Back, B.G. Glagola, H. Breuer, and V.E. Viola, Jr., Phys. Rev. C24 (1981) 89.
16. H. Yamada, D.R. Zolnowski, S.E. Cala, A.C. Kahler, J. Pierce, and T.T. Sugihara, Phys. Rev. Lett. 43 (1979) 605.
17. K. Goeffroy-Young, D.G. Sarantites, J.R. Beene, M.L. Halbert, D.C. Hensley, R.A. Davras, and J.H. Barker, Phys. Rev. C23 (1981) 2479.
18. J.P. Bondorf, J.N. De, G. Fai, A.O.T. Karvinen, and B. Jakobsson, Phys. Lett. 84B (1979) 162; J.P. Bondorf, J.N. De, G. Fai, A.O.T. Karvinen, B. Jakobsson and J. Randrup, Nucl. Phys. A333 (1980) 285.
19. K. Siwek-Wilczynska, E.H. du Marchie van Voorthuysen, J. van Popta, R.H. Siemssen, and J. Wilczynski, Phys. Rev. Lett. 42 (1979) 1599 and Nucl. Phys. A330 (1979) 150.
20. J.H. Barker, J.R. Beene, M.L. Halbert, D.C. Hensley, M. Jääskeläinen, D.G. Sarantites, and R. Woodward, Phys. Rev. Lett. 45 (1980) 424.
21. B.B. Back, K.L. Wolf, A.C. Mignerey, C.K. Gelbke, T.C. Aves, H. Breuer, V.E. Viola, Jr., and P. Dyer, Phys. Rev. C22 (1980) 1927.
22. W.G. Lynch, L.W. Richardson, M.B. Tsang, R.E. Ellis, C.K. Gelbke, and R.E. Warner, Phys. Lett. 108B (1982) 274.
23. I. Tanihata, S. Nagamiya, S. Schnetzer, and H. Steiner, Phys. Lett. 100B (1981) 121.
24. I. Tanihata, M.-C. Lemaire, S. Nagamiya, and S. Schnetzer, Phys. Lett. 97B (1980) 363.
25. J. Knoll and J. Randrup, Phys. Lett. 103B (1981) 264.
26. J. Knoll, Phys. Rev. C20 (1979) 773.
27. S.E. Koonin, Phys. Lett. 70B (1977) 43.
28. F. Zarbakhsh, A.L. Sagale, F. Brochard, T.A. Mulera, V. Perez-Mendez, R. Talaga, I. Tanihata, J.B. Carroll, K.S. Ganezer, G. Igo, J. Oostens, D. Woodard, and R. Sutter, Phys. Rev. Lett. 46 (1981) 1268.